Remodeling of Hippocampal Synapses After Hippocampus-Dependent Associative Learning

Geinisman, Yuri; Disterhoft, John F.; Gundersen, Hans Jørgen G.; McEchron, Matthew D.; Persina, Inna S.; Power, John M.; van der Zee, Eelke; West, Mark J.

Published in:
The Journal of Comparative Neurology

DOI:
10.1002/(SICI)1096-9861(20000131)417:1<49::AID-CNE4>3.0.CO;2-3

Publication date:
2000

THE JOURNAL OF COMPARATIVE NEUROLOGY 417:49–59 (2000)

Remodeling of Hippocampal Synapses After Hippocampus-Dependent Associative Learning

YURI GEINISMAN,*[1] JOHN F. DISTERHOFT,[1] HANS JØRGEN G. GUNDERSEN,[2] MATTHEW D. MCECHRON,[1] INNA S. PERSINA,[1] JOHN M. POWER,[1] EDDY A. VAN DER ZEE,[1] AND MARK J. WEST[3]

[1]Department of Cell and Molecular Biology, Northwestern University Medical School, Chicago, Illinois 60611

[2]Stereological Research Laboratory, University of Aarhus, 8000 Aarhus C, Denmark

[3]Institute for Neurobiology, University of Aarhus, 8000 Aarhus C, Denmark

ABSTRACT

The aim of this study was to determine whether hippocampus-dependent associative learning involves changes in the number and/or structure of hippocampal synapses. A behavioral paradigm of trace eyeblink conditioning was used. Young adult rabbits were given daily 80 trial sessions to a criterion of 80% conditioned responses in a session. During each trial, the conditioned (tone) and unconditioned (corneal airpuff) stimuli were presented with a stimulus-free or trace interval of 500 msec. Control rabbits were pseudoconditioned by equal numbers of random presentations of the same stimuli. Brain tissue was taken for morphological analyses 24 hours after the last session. Synapses were examined in the stratum radiatum of hippocampal subfield CA1. Unbiased stereological methods were used to obtain estimates of the total number of synapses in this layer as well as the area of the postsynaptic density. The data showed that the total numbers of all synaptic contacts and various morphological subtypes of synapses did not change in conditioned animals. The area of the postsynaptic density, however, was significantly increased after conditioning in axospinous nonperforated synapses. This structural alteration may reflect an addition of signal transduction proteins (such as receptors and ion channels) and the transformation of postsynaptically silent synapses into functional ones. The findings of the present study indicate that cellular mechanisms of hippocampus-dependent associative learning include the remodeling of existing hippocampal synapses. Further studies examining various time points along the learning curve are necessary to clarify the issue of whether these mechanisms also involve the formation of additional synaptic contacts. J. Comp. Neurol. 417: 49–59, 2000.

Indexing terms: structural synaptic plasticity; trace eyeblink conditioning; unbiased stereology; postsynaptic density; silent synapses; rabbit hippocampus

Cellular mechanisms of learning and memory have long been believed to include alterations in synapse number and structure (Ramón y Cajal, 1893; Tanzi, 1893). The validity of this notion was explored in a number of quantitative electron microscopic studies of the vertebrate brain (for reviews see Greenough and Bailey, 1988; Bailey and Kandel, 1993). The vast majority of the previous studies reported that the numerical density of synapses was increased as a consequence of learning of new behaviors. This was the most consistent observation, even though the effect of a variety of behavioral tasks was evaluated and the synapses were quantified in different brain regions.

Several groups have attempted to detect learning-induced changes in synapse number in the hippocampal formation, which is a brain region that is crucially important for certain forms of learning and memory (Wallenstein et al., 1998). Increases in the synaptic numerical

Grant sponsor: NIH/NINDS; Grant number: 5 RO1 NS34582; Grant sponsor: National Institutes of Health/National Institute on Aging; Grant number: 1 RO1 AG17139.

Dr. Persina's current address is: Department of Psychiatry and Behavioral Sciences, The Chicago Medical School, North Chicago, IL 60064.

Dr. Van Der Zee's current address is: Department of Zoology, University of Groningen, 9751 NN Haren, The Netherlands.

*Correspondence to: Dr. Yuri Geinisman, Department of CM Biology, Northwestern University Medical School, 303 East Chicago Avenue, Chicago, IL 60611. E-mail: yurig@nwu.edu

Received 2 February 1999; Revised 7 October 1999; Accepted 13 October 1999

density per unit area have been found to occur in the stratum radiatum of the CA1 subfield of the rat hippocampus after brightness discrimination conditioning (Wenzel et al., 1980) and in the molecular layer of the rat dentate gyrus after one-way active avoidance conditioning (Van Reempts et al., 1992). The numerical density of dendritic spines per unit volume has also been determined to increase in the molecular layer of the rat dentate gyrus after passive avoidance conditioning (O'Malley et al., 1998). In contrast, spatial learning in the Morris water maze has been demonstrated to have no effect on the synaptic numerical density per unit volume in the rat CA1 stratum radiatum and dentate gyrus molecular layer (Rusakov et al., 1997). Because of the discrepancies in the data regarding learning-induced alterations in the numerical density of synapses in the hippocampal formation, we decided to determine, with the aid of modern stereological approaches, whether hippocampus-dependent associative learning is accompanied by changes in the number and structure of hippocampal synapses.

The behavioral paradigm of trace eyeblink conditioning was used in our study because it is a form of associative learning that is known to depend on the structural integrity of the hippocampal formation. This brain region is involved most critically in associative learning and memory when the events that must be associated together are discontiguous, i.e., do not overlap in terms of their temporal and spatial positioning (for a review see Wallenstein et al., 1998). With the trace eyeblink paradigm, the conditioned stimulus (tone) not only precedes the unconditioned stimulus (airpuff), but is also separated from it by a stimulus-free, or "trace," interval. Correspondingly, lesions of the hippocampus have been shown to prevent acquisition of the trace eyeblink conditioned response in rabbits (Solomon et al., 1986; Moyer et al., 1990; Kim et al., 1995).

Electrophysiologically, it has been demonstrated that trace eyeblink conditioning in rabbits is accompanied by increases in the synaptic responsiveness (Power et al., 1997) and the postsynaptic excitability (DeJonge et al., 1990; Moyer et al., 1996) of CA1 pyramidal neurons. The excitability of the neurons is maximally enhanced 24 hours after learning (Moyer et al., 1996). At this time point, the immunoreactivity of PKCγ (i.e., γ-isoform of Ca^{2+}-dependent protein kinase C) has also been shown to increase in the rabbit hippocampus (Van der Zee et al., 1997). The learning-induced change in this enzyme, which has been implicated in synaptic plasticity, involves the apical dendrites of CA1 pyramidal cells in the CA1 stratum radiatum.

Based on these data, synapses were analyzed morphologically in the rabbit CA1 stratum radiatum 24 hours after trace eyeblink conditioning. The total number of synapses in this layer and the area of their postsynaptic density (PSD) were estimated, using unbiased sampling and counting procedures of modern stereology (Cruz-Orive and Weibel, 1990; Mayhew and Gundersen, 1996; Howard and Reed, 1998; West, 1999). Each conditioned animal was compared to a pseudoconditioned one that received an equal number of the conditioned and unconditioned stimuli presented in a random order. This provided an adequate control for possible activity-dependent structural alterations.

We report here that trace eyeblink conditioning is followed by an enlargement of the PSD area in axospinous nonperforated synapses, but does not involve a change in the total number of synaptic contacts in the CA1 stratum radiatum 24 hours after behavioral acquisition to a learning criterion. These data have been published in an abstract form (Geinisman et al., 1998).

MATERIALS AND METHODS

Experimental animals and behavioral training

Female New Zealand albino rabbits (*Oryctolagus cuniculus*), 8–10 weeks of age, were purchased from Hazelton Rabbitry (Denver, PA). Animal care was approved and managed by Northwestern University's Animal Care and Use Committee in compliance with National Institutes of Health guidelines. An important characteristic of female rabbits is the absence of the estrous cycle. These animals are induced ovulators, and their ovulation-provoking surges of luteinizing hormone are generated by mating (Hill and Wyse, 1989). Therefore, it was not necessary to control for the hormonal stage of the female rabbits examined.

The animals were trained in pairs and received either trace eyeblink conditioning or, as a control, pseudoconditioning according to an established experimental protocol (Moyer et al., 1990, 1996; Power et al., 1997; Van der Zee et al., 1997; DeJonge et al., 1990). Conditioned rabbits were given an 80-trial session per day until they reached a criterion of 80% conditioned responses during a session. To reach criterion, 5–10 training sessions were required. During each trial, the conditioned stimulus (CS; 100 msec, 85 dB, 6 kHz tone) and the unconditioned stimulus (US; 150 msec, 3.0-psi corneal airpuff) were presented with an intervening trace interval of 500 msec. An eyeblink response was considered to be conditioned if it occurred after CS onset and before US onset. Pseudoconditioned rabbits that received random presentations of the CS and US were trial- and session-matched with conditioned rabbits. Nine pairs of conditioned and pseudoconditioned animals were examined morphologically. Protocols for perfusion fixation, tissue processing, unbiased sampling, and counting have been described in detail elsewhere (Geinisman et al., 1996a), and they were followed in this work.

Tissue fixation and processing

Brain tissue was taken for morphological analyses 24 hours after the last training session. Animals were deeply anaesthetized with a combination of xylazine (6 mg/kg, i.m.) and ketamine hydrochloride (45 mg/kg, i.m.) followed 15 minutes later by pentobarbital sodium (75 mg/kg, i.m.). Transcardiac perfusion was then performed in three consecutive steps: (1) phosphate-buffered saline (pH = 7.3) containing heparin sodium (10 U/ml) injected at a rate of 50 ml/minute for 45 seconds (~40 ml); (2) 1% paraformaldehyde, 1.25% glutaraldehyde, and 0.02 mM $CaCl_2$ in 0.12 M phosphate buffer, pH = 7.3, perfused initially at a rate of 50 ml/minute for 10 minutes (500 ml) and thereafter at a rate of 25 ml/minute for additional 20 minutes (500 ml); (3) the same fixative at twice the aldehyde concentration delivered at a rate of 25 ml/minute for 12 minutes (300 ml). All solutions were warmed to 37°C and administered with a peristaltic pump. After the perfusion, animals were placed in sealed plastic bags and kept in a refrigerator for 2 hours at 4°C. The brain was then removed and the left

hemisphere postfixed in the double strength fixative at 4°C overnight.

After postfixation, the left hippocampal formation was dissected free, physically straightened to diminish its natural curvature (Gaarskjaer, 1978), and cut, perpendicular to its septotemporal axis, into 11–14 consecutive slabs using a tissue chopper equipped with a microdrive. The position of the first cut within the first 1.5-mm interval from the septal pole was determined randomly and the subsequent cuts were placed at a uniform interval of 1.5 mm from each other. The slabs obtained from each pair of conditioned and pseudoconditioned animals were coded and simultaneously processed for microscopy. Tissue was rinsed in cold 0.12 M phosphate buffer, treated with OsO_4 (2% solution in 0.12 M phosphate buffer for 90 minutes at 4°C) and rinsed again in the buffer at room temperature. Subsequently, the slabs were dehydrated in ethanol solutions of increasing concentrations, treated with propylene oxide, left overnight in a mixture (1:1) of propylene oxide–Araldite 502, flat embedded in Araldite using disk block embedding molds, and cured in an oven at 60°C for 48 hours.

Estimation of the total volume of the CA1 stratum radiatum

The total volume of the CA1 stratum radiatum was estimated by point counting at the light microscopic level, according to the Cavalieri principle. Because it could not be assumed that the thickness of the slabs was unaltered during the embedding procedure, the slab thickness was measured using an inverted microscope equipped with an eyepiece micrometer at a total magnification of 18×. Histological sections (3-μm-thick) were then prepared from the septal face of each tissue slab, so that the distance between the sections was equal to the thickness of the embedded slabs.

The borders of the CA1 subregion of the rabbit hippocampus could be reliably delineated in such sections stained with azure II–methylene blue. Although the CA1 subregion is continuous with the CA2 subfield and subicular complex, it can be unequivocally distinguished from these two hippocampal subdivisions. The giant pyramidal cells, typical of the CA3 subfield, are also present in the CA2 pyramidal layer, but are never observed in the CA1 stratum pyramidale, which contains relatively small pyramidal cells (Hjorth-Simonsen and Zimmer, 1975; Hjorth-Simonsen, 1977). The CA1 border with the subicular complex is clearly demarcated by an abrupt termination of a bundle of perforant path fibers that pass through the CA1 subregion (Lorento de Nó, 1934). Within this subregion, the extent of the stratum radiatum is limited by the stratum pyramidale on one side and bundle of perforant path fibers on the other (Hjorth-Simonsen and Zimmer, 1975).

Sectional profiles of the CA1 stratum radiatum were delineated according to the boundaries specified above and their outlines were drawn with the aid of a projection microscope at a final magnification of 41×. The area of each sectional profile was estimated by point counting. A transparent lattice of counting points that had a quadratic arrangement was randomly placed over an outline of a sectional profile. The number of points falling on the profile was counted. The density of points in the lattice was adjusted so that a total of 120–150 points would hit the entire set of sectional profiles. The total volume of the CA1 stratum radiatum was calculated as the product of the sum of points hitting the entire set of sectional profiles, the tissue area associated with each point, and the average slab thickness.

Selection of fields in which to sample synapses

Synapses were sampled with an equal probability along all three axes of the CA1 stratum radiatum. Sampling was performed randomly along the septotemporal axis (by virtue of preparing ultrathin sections from the same face of tissue slabs that were cut in a uniform random fashion) and in a systematic random manner along the other two axes of the CA1 stratum radiatum. For practical reasons, it was decided to limit the number of sampling fields to six per animal.

Initially, the location of the sampling fields was determined along the CA2–subicular axis. The length of the CA1 stratum radiatum along this axis was measured on each drawing of sectional profiles. The cumulative length was then calculated and divided into six uniform intervals. The lateral edge of each sampling field was marked on a profile drawing at the defined interval after random placement within the first interval. The markings were straight lines that crossed the width of the CA1 stratum radiatum in a direction perpendicular to the CA2–subicular axis and parallel to the cell body–apical dendrite axis.

In the next step, the location of the sampling fields along the cell body–apical dendrite axis was determined using a subset of six selected sectional profiles that represented six different tissue slabs. Each of these profiles was marked by a straight line drawn along the cell body–apical dendrite axis as indicated above. The length of the lines was measured on profile drawings, and the cumulative length was calculated and divided into six uniform intervals. Positions of the proximal (in relation to the pyramidal cell bodies) edges of the sampling fields were marked on profile drawings at the defined intervals after a random placement within the first interval.

Each selected slab was trimmed down to prepare a series of 31–38 consecutive ultrathin sections from the septal slab face. The first trimming cut, which formed the lateral edge of a sampling field, was made according to its position indicated on a sectional profile drawing in relation to the surrounding blood vessels. The following trimming cuts were made so as to prepare sections that had the shape of a trapezoid with its longest side formed by the first cut. The ultrathin sections spanned the entire width of the CA1 stratum radiatum, from the stratum pyramidale to the bundle of perforant path fibers. Each series of ultrathin sections was counterstained with uranyl acetate and lead citrate, mounted on a single-slot grid coated with collodion-carbon, and used to obtain electron micrographs of a sampling field.

At the electron microscopic level, two edges of a given sampling field were identified to determine its location in ultrathin sections. The lateral edge was demarcated by the long side of the section, and the proximal edge was defined by its distance from the pyramidal cell layer. This distance was initially measured on the drawings of the sectional profiles and then assessed in the electron microscope with the aid of the field delineator of the microscope screen. Because a sampling field had to be photographed in corresponding parts of consecutive ultrathin sections in

a series, only straight ribbons of ultrathin sections were used. The sections were aligned by placing a prominent tissue landmark (such as a transversely sectioned myelinated fiber) on the same position on the microscope screen. Electron micrographs were taken at an initial magnification of 8,000× and enlarged photographically to a final magnification of 20,000×. At this final magnification, all synaptic contacts could be unequivocally identified and a relatively large number of synapses could be sampled. A magnification standard (grating replica) was photographed and printed with each series of electron micrographs.

Synapse counting with disectors

The stereological disector technique (Sterio, 1984; Gundersen, 1986) was used to count synapses. Each disector consisted of micrographs of two adjacent ultrathin sections, a reference section, and a look-up section immediately above it. A transparency with an unbiased counting frame (Gundersen, 1977) was superimposed over a reference section micrograph. The edges of the frame and micrograph were separated by a distance (guard area) that exceeded the largest linear dimension of the largest PSD profile. Synapses were identified on the reference section micrograph, with the aid of micrographs of adjacent serial sections, by the presence of synaptic vesicles and a PSD, the latter being used as a counting unit. Then synapses were labeled on the reference section micrograph if their PSD profiles were located either entirely or partly within the frame and did not intersect the forbidden edges of the frame and their extensions. Two or more profiles belonging to the same PSD of a perforated synapse were connected by an imaginary straight line and treated as a single entity. Finally, only those labeled synapses that had a PSD profile in the reference, but not in the look-up, section were counted. The last 8–10 sections of each series were not used as disectors to ensure that PSDs of all sampled synapses were included in their entirety in the section series.

Estimation of the numerical density and the total number of synapses in the CA1 stratum radiatum

To estimate the synaptic numerical density per unit volume, it is necessary to know the volume of the disector. This volume is limited by the counting frame area and the disector height, which is the distance between corresponding surfaces of the two sections. When the disector consists of two immediately adjacent sections, its height is equal to the thickness of the reference section. The section thickness was estimated with Small's method of minimal folds as described by Weibel (1979) and Royet (1991) because this method provides accurate estimates of section thickness compared with other techniques (Calverley et al., 1988; De Groot, 1988; Hunter and Stewart, 1989). A minimal fold is an artifact formed by a slight pinching of a section. Because the minimal fold stands upright, its width is equal to twice the section thickness. Minimal folds were photographed at a magnification of 100,000× and their width was measured directly on the negatives. Some ultrathin sections of each series did not contain minimal folds. Therefore, the mean section thickness of all those sections that contained minimal folds was used to calculate the height of the disectors.

The mean area of the unbiased counting frame was 79.0 μm^2, the mean disector height was 0.080 μm, and the mean disector volume was 6.32 μm^3. The latter value was used to calculate the numerical density of synapses per unit volume as the quotient of the mean number of synapses counted per disector and the mean volume of the disectors. The total number of synapses in the total volume of the CA1 stratum radiatum was calculated as the product of the volume and synaptic numerical density.

Estimates of the total number of synaptic contacts reported here were made by counting axospinous perforated and axodendritic synapses with 144 disectors (24 disectors per serially sectioned field) and axospinous nonperforated synapses with 18 disectors (3 disectors per field) in each animal. This resulted in relatively large samples of axospinous perforated synapses (102–221, mean = 159) and axospinous nonperforated synapses (133–175, mean = 154) per animal. The size of the sample of axodendritic synapses was smaller (11–36, mean = 26). Additionally, estimates of total number were also obtained separately for each of the following morphological categories of synapses: (1) all axospinous; (2) axospinous nonperforated; axospinous perforated with (3) fenestrated, (4) horseshoe-shaped, and (5) segmented PSDs, (6) multiple transmission zones or (7) spine partitions; (8) axospinous with a postsynaptic concavity of the synaptic apposition zone; and (9) axodendritic asymmetrical synapses. There was an overlap between some synaptic categories. A proportion of synapses with fenestrated, horseshoe-shaped, and segmented PSDs was included in the category characterized by the presence of spine partitions. Similarly, some perforated and nonperforated axospinous synapses also belonged to the category exhibiting a postsynaptic concavity.

Estimation of the PSD area

The length of PSD profiles (Fig. 1) was measured (at an additional magnification of 5×) on electron micrographs of consecutive serial sections through each sampled synapse to estimate the PSD area. Biases related to overprojection (i.e., apparent enlargement of opaque profile images because of the finite thickness of transparent sections) were taken into account by subtracting the maximal profile length from the sum of lengths of all sectional profiles belonging to a given PSD (cf. Gundersen, 1986). The area of the PSD was estimated as $a_i = (4\bar{t}/\pi)(\Sigma\ell_i - \max\ell_i)$, where ℓ_i is the length of each PSD sectional profile in the ith synapse, $\max\ell_i$ is the PSD maximal profile length, $\bar{t}$ is the average section thickness, and $4/\pi$ is the factor that makes the area estimate correct for isotropically oriented PSDs. In those rare cases (1:555) when a PSD was visible in only one section, its area was estimated as $a_i = 0$. For axospinous perforated synapses that have a PSD consisting of two or more distinct segments, the area of the PSD plate was determined separately for each individual segment as indicated above. The sum of the individual values was used as an estimate of the total area of the entire segmented PSD. For other axospinous perforated synapses, the length of each discontinuous PSD profile was expressed as the sum of lengths of its separate fragments.

Statistical treatment of the data

Differences between conditioned and pseudoconditioned animals, with regard to the volume of the CA1 stratum radiatum, the number of synapses in this layer, and the

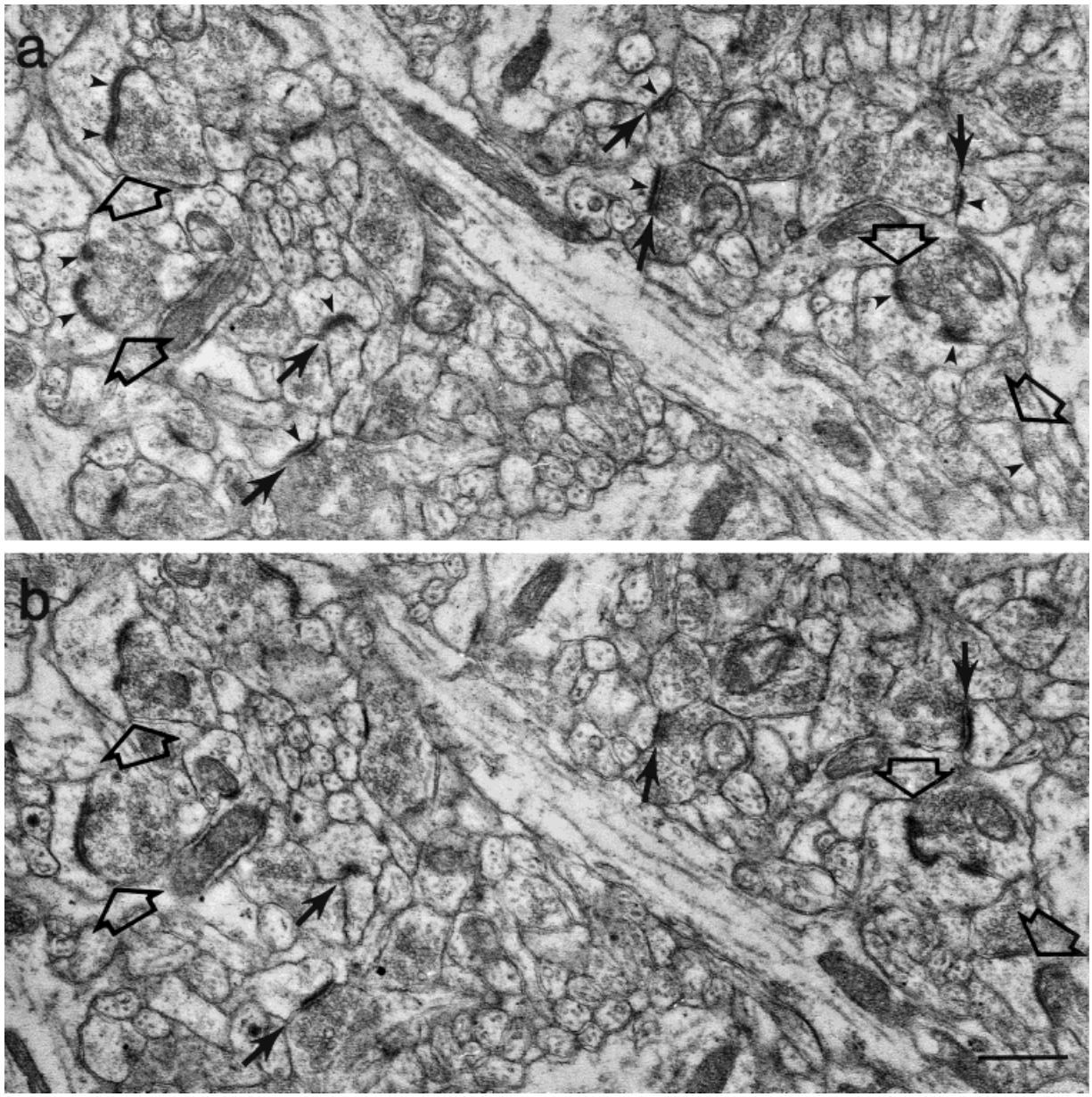

Fig. 1. Electron micrographs of consecutive serial sections (**a,b**) show the neuropil in the rabbit CA1 stratum radiatum. Representative axospinous perforated and nonperforated synapses are indicated by open and closed arrows, respectively. Profiles of the postsynaptic densities in these synapses are marked by arrowheads in (a). Scale bar = 0.5 μm.

area of their PSDs, were examined for statistical significance. Tests for matched pairs were used because of the paired design of the behavioral experiment. Conditioned and pseudoconditioned rabbits were trained in pairs on the same days. Furthermore, animals in each pair received the same numbers of daily training sessions and the same numbers of the conditioned and unconditioned stimuli. These were different for different pairs because of a variation in the rate of reaching the behavioral criterion among conditioned animals.

Individual estimates of the mean total number of synapses belonging to a given morphological category and of the mean area of their PSDs were used as the units of observation. Mean values tend to be distributed normally. Moreover, initial analyses of heterogeneity of variances with the test for dependent samples (Howell, 1982) showed that differences between the variances of the group means were not significant for the comparison of CA1 stratum radiatum volumes, for most (10 of 12) comparisons of synapse numbers and for all comparisons of PSD areas. For these reasons, the t-test for matched pairs was used for the statistical treatment of the data with the exception of the following two cases. The heterogeneity of variance test for dependent samples reached significance for only those two subtypes of axospinous perforated synapses that exhibited a horseshoe-shaped PSD (t = 2.244,

TABLE 1. Total Volume of the CA1 Stratum Radiatum and the Total Number of Synapses in This Layer in Conditioned (CD) and Pseudoconditioned (PC) Rabbits[1]

Pair of animals	Total volume (mm^3)			Total number of synapses ($\times 10^6$)		
	CD rabbits	PC rabbits	ΔCD-PC	CD rabbits	PC rabbits	ΔCD-PC
1	14.4	16.5	−2.1	20,980	23,480	−2,500
2	16.7	15.4	1.3	26,039	22,727	3,312
3	15.9	15.7	0.2	25,614	26,740	−1,126
4	17.4	13.3	4.1	25,736	22,228	3,508
5	14.1	15.8	−1.7	23,116	24,776	−1,660
6	15.4	16.6	−1.2	24,774	25,407	−633
7	14.9	12.8	2.1	21,923	22,222	−299
8	14.0	15.6	−1.6	23,582	24,084	−502
9	12.7	11.7	1.0	17,639	17,588	51
Mean	15.1	14.8	0.233	23,250	23,267	16.8
SE	0.487	0.587	0.695	915	869	690
P			0.746			0.981

[1]ΔCD-PC, differences between values estimated for paired conditioned and pseudoconditioned rabbits; *P*, significance of differences between the groups of conditioned and pseudoconditioned rabbits evaluated with the two-tailed *t*-test for matched pairs.

$df = 7, P < 0.05$) or spine partitions ($t = 2.226$, $df = 7, P < 0.05$). In these two cases, the data were analyzed with the Wilcoxon signed rank test for matched pairs because it is a nonparametric test that does not rely on an assumption about the equality of variances in the populations from which the samples under comparison were drawn.

The present study included an examination of various morphological subtypes of synapses. For this reason, multiple paired t-tests were used. Statistical analyses involving multiple t-tests are known to increase the probability of a type I statistical error. Therefore, when a difference between conditioned and pseudoconditioned animals on the morphological measures used was found to be statistically significant with the paired t-test, a Bonferroni correction for the level of significance was applied to reduce the probability of a type I statistical error.

RESULTS

Inspection of electron micrographs of serial sections revealed that the synaptic population of the CA1 stratum radiatum consists of axodendritic synapses on dendritic shafts and axospinous synapses on dendritic spines. Axodendritic synapses are encountered rarely, and the vast majority (98%) of synaptic contacts belong to the axospinous category. Axospinous junctions may be subdivided into large perforated synapses, which exhibit a discontinuous PSD profile in at least one serial section, and small nonperforated synapses, which show a continuous PSD profile in all consecutive sections (Fig. 1).

Stability of total synapse number in the CA1 stratum radiatum after trace eyeblink conditioning

Axospinous perforated and nonperforated synapses, as well as axodendritic junctions, were quantified separately, and their total numbers were added together to obtain unbiased estimates of the total number of all synapses in the CA1 stratum radiatum. The results showed that the total volume of the CA1 stratum radiatum and the total number of synapses in this layer were virtually the same in conditioned and pseudoconditioned animals (Table 1). The group means of the total number of synapses differed by 0.07%, demonstrating that trace eyeblink conditioning is not accompanied by a net increase in synapse number 24 hours after successful acquisition of the conditioned response.

Because the total number of synaptic contacts was not altered by conditioning, it was deemed appropriate to test the hypothesis (Tanzi, 1893) that learning-induced remodeling of existing synapses was involved. Initially, we explored the possibility that some morphological subtypes of synapses had been transformed into other, presumably more efficacious subtypes. It has previously been reported that the numerical density of certain synaptic subtypes increases after learning (Vrensen and Nunes Cardozo, 1981; Van Reempts et al., 1992) and the induction of hippocampal long-term potentiation (Lee et al., 1980; Chang and Greenough, 1984; Desmond and Levy, 1986; Schuster et al., 1990; Geinisman et al., 1993, 1996b; Buchs and Muller, 1996). Quantitative analyses of the synaptic subtypes implicated in learning- and LTP-induced plasticity revealed that their total numbers did not change significantly after trace eyeblink conditioning (Table 2).

Enlargement of the PSD area in axospinous nonperforated synapses after trace eyeblink conditioning

The other possibility explored was that synaptic transmission zones, which are delineated postsynaptically by the PSD, enlarge as a consequence of conditioning. The results of previous studies based on the analysis of single sections have indicated that the length of PSD profiles increases after acquisition of a new behavior (DeVoogd et al., 1985; Horn et al., 1985; Van Reempts et al., 1992; Stewart and Rusakov, 1995). We measured the length of

TABLE 2. Group Means (± SE) of Total Synapse Number Estimated for Various Morphological Categories of Synaptic Contacts in the CA1 Stratum Radiatum of Conditioned (CD) and Pseudoconditioned (PC) Rabbits

Synapse category	Mean synapse number ($\times 10^6$)	
	CD group	PC group
All axospinous	22,809 ± 911	22,851 ± 843
All axospinous perforated	2,443 ± 131	2,734 ± 214
Axospinous perforated		
with a fenestrated PSD[1]	712 ± 70	894 ± 95
with a horseshoe-shaped PSD	938 ± 42	1.028 ± 89
with a segmented PSD	793 ± 61	811 ± 80
with multiple transmission zones	690 ± 156	698 ± 64
with spine partitions	1,487 ± 83	1,666 ± 177
Axospinous with a postsynaptic concavity	4,406 ± 284	4,519 ± 330
All axodendritic	458 ± 41	399 ± 48
Axodendritic asymmetrical	279 ± 36	239 ± 35

[1]PSD, postsynaptic density.

TABLE 3. Total Number of Axospinous Nonperforated Synapses in the CA1 Stratum Radiatum and the Area of the PSD in These Synapses in Conditioned (CD) and Pseudoconditioned (PC) Rabbits[1]

Pair of animals	Total number of synapses ($\times 10^6$)			Mean PSD area ($nm^2 \times 10^3$)		
	CD rabbits	PC rabbits	ΔCD-PC	CD rabbits	PC rabbits	ΔCD-PC
1	17,974	19,435	−1,461	32.1	26.5	5.6
2	23,048	20,171	2,877	33.9	30.7	3.2
3	22,084	22,358	−274	27.5	24.4	3.1
4	23,097	19,173	3,924	33.2	29.1	4.1
5	20,327	22,223	−1,896	27.0	29.2	−2.2
6	22,743	22,179	564	30.9	31.4	−0.5
7	18,992	19,690	−698	29.9	24.8	5.1
8	20,182	20,707	−525	29.5	24.9	4.6
9	14,848	15,119	−271	28.5	26.5	2.0
Mean	20,366	20,117	249	30.3	27.5	2.78
SE	923	751	646	0.814	0.886	0.873
P			0.710			0.0129

[1]For abbreviations see Table 1.

PSD profiles on electron micrographs of consecutive sections through each sampled synapse to obtain estimates of the PSD area. Initially, three primary subtypes of synaptic junctions, namely, axospinous perforated, axospinous nonperforated, and axodendritic synaptic contacts, were examined. It was found that PSDs of axospinous nonperforated synapses had a larger area in conditioned rabbits than in pseudoconditioned controls (Table 3). Evaluation of the data with the paired t-test showed that the difference between the group means was statistically significant ($P = 0.0129$). When a Bonferroni correction for multiple (n = 3) t-tests was applied, this difference still remained significant ($P < 0.05$).

Comparison of frequency distributions of nonperforated PSD areas in the conditioned and pseudoconditioned groups of animals demonstrated that an enlargement of the smallest nonperforated PSDs in conditioned rabbits accounted for the observed significant change. The proportion of nonperforated synapses with PSDs that fell into the smallest size category (PSD area $< 20\ nm^2 \times 10^3$) was decreased in the conditioned group (Fig. 2). The total number of nonperforated synapses was not altered by conditioning (Table 3) and, hence, the proportions of those nonperforated synaptic contacts that had PSDs belonging to larger size categories (PSD area $\geq 20\ nm^2 \times 10^3$) were increased in conditioned animals (Fig. 2). This PSD modification was estimated to involve $1{,}265 \times 10^6$ nonperforated synapses that constitute 5.4% of the total synaptic population in the CA1 stratum radiatum. Examination of the other morphological subtypes of synapses revealed no significant conditioning-related change in the area of their PSDs (Table 4).

It was necessary to determine whether the observed difference in the size of nonperforated PSDs between the two groups of animals under study was caused by an increase in the conditioned rabbits or to a decrease in the pseudoconditioned ones. For this purpose, a separate group of five unstimulated control rabbits was examined. The PSD area was estimated in nonperforated synapses from the CA1 stratum radiatum as specified above. The estimates of the area of nonperforated PSDs obtained from individual unstimulated animals (24.0, 24.5, 25.5 27.6, and 29.1 $nm^2 \times 10^3$) were within the range of those obtained from pseudoconditioned controls (Table 3). Analysis of variances, using a one-way analysis of variance with a correction for unequal sample sizes (Howell, 1982), showed that differences among unstimulated, pseudocon-

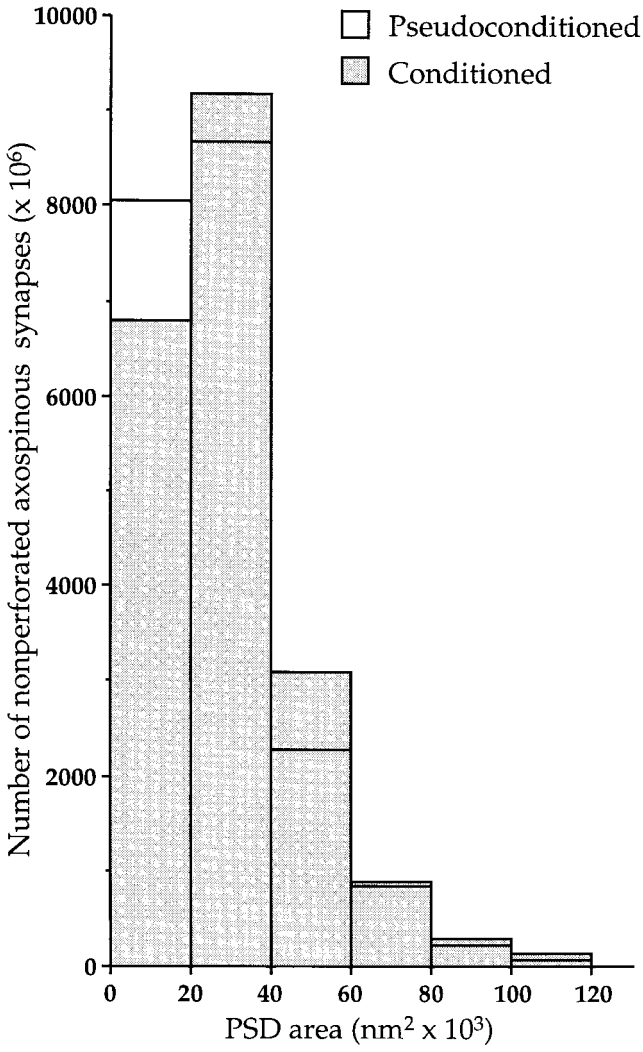

Fig. 2. Frequency distributions of postsynaptic density (PSD) areas in nonperforated axospinous synapses from the CA1 stratum radiatum of conditioned and pseudoconditioned groups of rabbits. The total number of nonperforated synapses is shown for each size category of their PSDs. It was calculated from the percentage of these synaptic contacts in a given category.

TABLE 4. Group Means (± SE) of the Postsynaptic Density Area Estimated for Various Morphological Categories of Synapses in the CA1 Stratum Radiatum of Conditioned (CD) and Pseudoconditioned (PC) Rabbits

	Mean PSD area ($nm^2 \times 10^3$)	
Synapse category	CD group	PC group
All axospinous perforated	86.0 ± 2.76	82.5 ± 2.62
Axospinous perforated		
with a fenestrated PSD[1]	88.2 ± 3.75	83.6 ± 3.38
with a horseshoe-shaped PSD	85.2 ± 3.06	78.3 ± 3.06
with a segmented PSD	85.5 ± 3.53	86.6 ± 2.94
with multiple transmission zones	85.6 ± 3.82	88.6 ± 2.75
with spine partitions	88.1 ± 2.85	87.7 ± 2.13
Axospinous with a postsynaptic concavity	84.8 ± 3.11	81.9 ± 2.42
All axodendritic	58.0 ± 2.74	63.6 ± 3.44
Axodendritic asymmetrical	65.4 ± 4.79	69.1 ± 3.86

[1]PSD, postsynaptic density.

ditioned, and conditioned rabbits with respect to the nonperforated PSD area were statistically significant [$F_{0.025}(2.20) = 5.23, P < 0.025$]. Post hoc comparison of the data with the Student–Newman–Keuls test revealed that the conditioned group was significantly different on this measure as compared with both the unstimulated and pseudoconditioned group. The difference between the latter two groups, however, was not significant. Accordingly, the mean values of the area of nonperforated PSDs estimated for the groups of unstimulated and pseudoconditioned animals (26.1 ± 0.964 and 27.5 ± 0.886 $nm^2 \times 10^3$, respectively) differed by only 5.4%. These data indicate that the relative enlargement of the nonperforated PSD area in conditioned animals, as compared to pseudoconditioned animals, represents a conditioning-induced increase in the PSD size.

DISCUSSION

The results presented here indicate that trace eyeblink conditioning is associated with remodeling of the PSD in existing synaptic contacts, but does not involve a change in the total number of synapses in the CA1 stratum radiatum of rabbits examined 24 hours after learning to a behavioral criterion. The increase in the PSD area observed after trace eyeblink conditioning may be related to an enhancement of the efficacy of synaptic transmission, which is believed to be necessary for learning (Tanzi, 1893; Hebb, 1975; Konorski, 1948). The PSD contains signal transduction proteins, such as postsynaptic receptors and ion channels (Ziff, 1997; Kennedy, 1998). The learning-induced enlargement in the PSD area may reflect an addition of these components and, hence, an augmentation of synaptic efficacy.

The recent discovery of "silent" synapses provides support for this supposition. Electrophysiological experiments have revealed that a high proportion of synaptic contacts in the rat CA1 stratum radiatum exhibit functional *N*-methyl-D-aspartate (NMDA) receptors, but not functional α-amino-3-hydroxy-5-methyl-4-isoxazoleproprionate (AMPA) receptors (Issac et al., 1995; Liao et al., 1995). This makes such synapses postsynaptically silent in that they do not generate a synaptic response to a release of a neurotransmitter at normal resting potentials. Immunocytochemical studies have also demonstrated that some hippocampal axospinous synapses exhibit only NMDA, but not AMPA, receptor immunoreactivity (Desmond and Weinberg, 1998; He et al., 1998; Petralia et al., 1999; Takumi et al., 1999). It is a lack of AMPA receptors and not their inactive state that accounts for this phenomenon (Nusser et al., 1998; Takumi et al., 1999). Of special importance is the observation that silent synapses acquire AMPA-type responses after induction of hippocampal long-term potentiation (LTP) (Issac et al., 1995; Liao et al., 1995), indicating that silent synapses may be transformed into active synaptic contacts as a result of LTP induction (Malenka and Nicoll, 1997). Because hippocampal LTP is widely regarded as a synaptic model of memory (Bliss and Collingridge, 1993), it seems reasonable to hypothesize that the same synaptic modification may take place as a consequence of hippocampus-dependent associative learning.

It has been demonstrated that the ratio between AMPA and NMDA receptors is directly proportional to the PSD size in axospinous nonperforated synapses from the rat CA1 stratum radiatum and that the AMPA receptor number regresses to zero when a PSD diameter is smaller than 180 nm (Takumi et al., 1999). This suggests that the PSD may increase in size because of the insertion of AMPA receptors, which is necessary for the silent synapses lacking these receptors to become active. Notably, only the smallest nonperforated PSDs were increased in their area in conditioned animals (Fig. 2). The observed enlargement of the PSD after trace eyeblink conditioning may therefore represent a structural correlate of the transformation of silent synapses into functional ones.

An intriguing observation made in our study is that the learning-induced increase in the PSD area selectively involved only nonperforated axospinous synapses. None of the other synaptic subtypes exhibited an alteration of this type. A characterization of nonperforated synaptic contacts provides a plausible explanation for this observation. An examination of axospinous synapses in the molecular layer of the rat dentate gyrus has shown that about 67% of nonperforated synapses do not exhibit AMPA receptor immunoreactivity, whereas the size of AMPA-immunonegative fraction of perforated synapses (~30%) is at least twice smaller (Desmond and Weinberg, 1998). In the rabbit CA1 stratum radiatum, the ratio of nonperforated to perforated synapses is 7.4:1 (compare Tables 2 and 3). Thus, the pool of silent axospinous synapses lacking AMPA receptors appears to consist primarily of those synaptic junctions that have a relatively small nonperforated PSD. Provided AMPA receptor clusters are inserted into PSDs of silent synaptic contacts after trace eyeblink conditioning, the resulting increase in the PSD area would be detected predominantly, if not exclusively, in nonperforated axospinous synapses.

In view of the above considerations, one would expect that an augmentation of synaptic transmission is likely to occur in the rabbit CA1 stratum radiatum after acquisition of the trace eyeblink conditioned response. Power et al. (1997) tested the validity of such a prediction. In their study, rabbits were conditioned according to the protocol described above. Dendritic field potentials were recorded extracellularly from the CA1 stratum radiatum in hippocampal slices after Schaffer collateral stimulation. The results showed that synaptic responses, as measured by the dendritic excitatory postsynaptic potential (EPSP) slope, were markedly and significantly augmented in conditioned animals 1 hour after the last training session relative to those recorded from pseudoconditioned or unstimulated controls. Although a clear trend toward an increase in the dendritic EPSP slope was observed 24 hours after conditioning, it was not statis-

tically significant. To determine whether this trend was a reflection of an actual change, an attempt was made to lower the interanimal variation by eliminating the variability stemming from differences among various cohorts of rabbits (J.M. Power, unpublished observations). The data were reexamined by comparing only those animals that belonged to the same cohort (i.e., that were delivered by the supplier at the same time and trained on the same days). Pseudoconditioned controls were not available for within-cohort comparisons. However, the EPSP slope values of the pseudoconditioned rabbits were identical to those of the unstimulated rabbits. When compared with unstimulated controls from the same cohort, conditioned animals showed a significant augmentation of synaptic responses 24 hours after reaching behavioral criterion. The magnitude of the change was the same as that estimated 1 hour after conditioning. Thus, acquisition of the trace eyeblink conditioned response is associated with an augmentation of impulse transmission at Schaffer collateral–CA1 pyramidal cell synapses. This learning-related synaptic enhancement appears to last for at least 24 hours after the cessation of training, and it was at 24 hours after the last training session that we observed the structural modification of nonperforated PSDs described here.

Our data demonstrating that associative learning does not involve an increase in the total number of synapses 24 hours after conditioning are in marked contrast with those of earlier electron microscopic studies of the vertebrate brain (Wenzel et al., 1980; Vrensen and Nunes Cardozo, 1981; DeVoogd et al., 1985; Stewart et al., 1987; Hunter and Stewart, 1989; Black et al., 1990; Van Reempts et al., 1992; Kleim et al., 1996, 1997; O'Malley et al., 1998). The previous studies reported learning-related increases in the numerical density of synapses, which in general has led to the conclusion that there is learning-induced synaptogenesis (Greenough and Bailey, 1988; Bailey and Kandel, 1993). This conclusion is consistent with the hypothesis (Ramón y Cajal, 1893) that structural substrates of learning may include the formation of additional synaptic contacts.

The discrepancy between the results reported here and those of the previous work may be explained in a number of ways. One of these is that various forms of learning may be accompanied by different patterns of structural synaptic alterations. Some forms of associative learning, such as trace eyeblink conditioning, may trigger a remodeling of existing synapses, whereas others may evoke a net synaptogenesis. Another possibility is that trace eyeblink conditioning may induce an increase in the total number of synapses in the CA1 stratum oriens, where the basal dendrites of CA1 pyramidal neurons are located, rather than in the CA1 stratum radiatum, which contains the apical dendrites. This supposition is compatible with the data obtained by means of confocal microscopy. Spatial training of rats was found to be followed by an increase in the number of spines on the basal dendrites of CA1 pyramidal cells with no change in the spine density on the apical dendrites (Moser et al., 1994; 1997). One more possibility is suggested by the dynamic nature of the learning phenomenon. Various phases of the acquisition/consolidation process may involve either a remodeling of synaptic contacts or a net synaptogenesis. In fact, there are data suggesting that changes in PSD dimensions may occur early after conditioning and may be followed later by an increase in the numerical density of synapses (Stewart and Rusakov, 1995). In our study, synapses were quantified only at one defined time point relative to behavioral acquisition. If stereological analyses were performed at various time points along the learning curve, an increase in synapse number resulting from trace eyeblink conditioning might have been detected as well.

It is also conceivable, however, that the results of some of the earlier quantitative electron microscopic studies were affected by the less robust methodology available at the time they were carried out. Uniform random sampling throughout the entire region of interest was not usually performed in these studies, and the sampling of synapses was confined only to a certain part of the region. Selective sampling of this type is potentially biased (Coggeshall and Lekan, 1996). It results in estimates that may be characteristic only of a subset of synapses in the regional segment selected for analyses. Moreover, most previous studies cited above used single ultrathin sections for identifying and counting synapses (Wenzel et al., 1980; Vrensen and Nunes Cardozo, 1981; DeVoogd et al., 1985; Stewart et al., 1987; Hunter and Stewart, 1989; Black et al., 1990; Van Reempts et al., 1992). An unequivocal identification of synapses can only be achieved when synaptic contacts are visualized in consecutive serial sections (Geinisman et al., 1996a). In addition, counts of synaptic profiles in single sections provide estimates of synapse number that may be biased by several factors, including the size, shape, and orientation of synaptic contacts, the section thickness, truncation, and overprojection (cf. Gundersen, 1986; West, 1993). The magnitude and direction of the biases may be different in conditioned and control animals. If various forms of learning involve an enlargement of the PSD, this may explain why the most consistent observation made in the earlier studies was an increase in the numerical density of synapses (Greenough and Bailey, 1988; Bailey and Kandel, 1993). Profiles of the larger PSDs would have been observed more frequently in single random sections than those of the smaller PSDs. Because the PSD was used to identify and count synapses, the estimates of synapse number would have been systematically larger in animals that had learned a given behavioral task than in the controls, even though there were no differences in the total number of synapses.

Another methodological problem of the earlier studies is that their results were most often expressed in terms of the number of synapses per unit area or volume of tissue (Wenzel et al., 1980; Vrensen and Nunes Cardozo, 1981; DeVoogd et al., 1985; Stewart et al., 1987; Hunter and Stewart, 1989; Van Reempts et al., 1992; Rusakov et al., 1997; O'Malley et al., 1998). Such density estimates, as opposed to those of the total number, are affected by changes in tissue volume that result from processing for microscopy. It was not determined, however, whether or not these changes were different in the conditioned and control animals examined. To circumvent this problem, the ratio of synapses to principal postsynaptic neurons was estimated in two recent studies (Kleim et al., 1996; 1997). Because both the principal neurons and the interneurons form postsynaptic elements in the regions examined, the latter approach relies on the unverified assumption that the number of synaptic contacts involving the interneurons is not altered by learning.

By using unbiased stereological methods to obtain estimates of total synapse number and PSD area, we have avoided many of the difficulties associated with the inter-

pretation of the data obtained with previously available methodologies. Here we present evidence that cellular mechanisms of hippocampus-dependent associative learning include the remodeling of existing hippocampal synapses. Further studies are necessary to elucidate the problem of whether these mechanisms also involve the formation of additional synaptic contacts.

ACKNOWLEDGMENTS

We thank R. W. Berry, M.-M. Mesulam, and E. Mugnaini of Northwestern University for critical review of the manuscript, and W. Goossens for skillful technical assistance.

LITERATURE CITED

Bailey CH, Kandel ER. 1993. Structural changes accompanying memory storage. Annu Rev Physiol 55:397–426.

Black JE, Isaaks KR, Anderson BJ, Alcantara AA, Greenough WT. 1990. Learning causes synaptogenesis, whereas motor activity causes angiogenesis, in cerebellar cortex of adult rats. Proc Natl Acad Sci USA 87:5568–5572.

Bliss TVP, Collingridge GL. 1993. A synaptic model of memory: long-term potentiation in the hippocampus. Nature 361:31–39.

Buchs P-A, Muller D. 1996. Induction of long-term potentiation is associated with major ultrastructural changes of activated synapses. Proc Natl Acad Sci USA 93:8040–8045.

Calverley PKS, Bedi KS, Jones DG. 1988. Estimation of the numerical density of synapses in rat neocortex. Comparison of the "disector" with an "unfolding" method. J Neurosci Methods 23:195–205.

Chang F-L, Greenough WT. 1984. Transient and enduring morphological correlates of synaptic activity and efficacy change in the rat hippocampal slice. Brain Res 309:35–46.

Coggeshall RE, Lekan HA. 1996. Methods for determining numbers of cells and synapses: a case for more uniform standards of review. J Comp Neurol 364:6–15.

Cruz-Orive LM, Weibel ER. 1990. Recent stereological methods for cell biology: a brief survey. Am J Physiol 258:L148–L156.

De Groot DMG. 1988. Comparison of methods for the estimation of the thickness of ultrathin tissue sections. J Microsc (Lond) 151:23–42.

DeJonge MC, Black J, Deyo RA, Disterhoft JF. 1990. Learning-induced afterhyperpolarization reductions in hippocampus are specific for cell type and potassium conductance. Exp Brain Res 80:456–462.

Desmond NL, Levy WB. 1986. Changes in the numerical density of synaptic contacts with long-term potentiation in the hippocampal dentate gyrus. J Comp Neurol 253:466–475.

Desmond NL, Weinberg RJ. 1998. Enhanced expression of AMPA receptor protein at perforated axospinous synapses. NeuroReport 9:857–860.

DeVoogd TJ, Nixdorf B, Nottenbohm F. 1985. Synaptogenesis and changes in synaptic morphology related to acquisition of new behavior. Brain Res 329:304–308.

Gaarskjaer FB. 1978. Organization of the mossy fiber system of the rat studied in extended hippocampi. I. Terminal area related to number of granule and pyramidal cells. J Comp Neurol 178:49–72.

Geinisman Y, deToledo-Morrell L, Morrell F, Heller RE, Rossi M, Parshall RF. 1993. Structural synaptic correlate of long-term potentiation: formation of axospinous synapses with multiple, completely partitioned transmission zones. Hippocampus 3:435–446.

Geinisman Y, Gundersen HJG, Van der Zee E, West MJ. 1996a. Unbiased stereological estimation of the total number of synapses in a brain region. J Neurocytol 25:805–819.

Geinisman Y, deToledo-Morrell L, Morrell F, Persina IS, Beatty MA. 1996b. Synapse restructuring associated with the maintenance phase of hippocampal long-term potentiation. J Comp Neurol 368:413–423.

Geinisman Y, Disterhoft JF, Gundersen HJG, McEchron MD, Persina IS, Power JM, Van der Zee EA, West MJ. 1998. Trace eyeblink conditioning induces a restructuring of preexisting synapses, rather than synaptogenesis. Soc Neurosci Abstr 24:1422.

Greenough WT, Bailey CH. 1988. The anatomy of a memory: convergence of results across a diversity of tests. Trends Neurosci 11:142–147.

Gundersen HJG. 1977. Notes on the estimation of the numerical density of arbitrary profiles: the edge effect. J Microsc (Lond) 111:219–223.

Gundersen HJG. 1986. Stereology of arbitrary particles. A review of unbiased number and size estimators and the presentation of some new ones, in memory of William R. Thompson. J Microsc (Lond) 143:219–223.

He Y, Janssen WJM, Morrison, JH. 1998. Synaptic coexistence of AMPA and NMDA receptors in the rat hippocampus: a postembedding immunogold study. J Neurosci Res 54:444–449.

Hebb DO. 1975. The organization of behavior. New York: John Wiley & Sons.

Hill RW, Wyse GA. 1989. Animal physiology, 2nd ed. New York: Harper & Row.

Hjorth-Simonsen A. 1977. Distribution of commissural afferents to the hippocampus of the rabbit. J Comp Neurol 176:495–514.

Hjorth-Simonsen A, Zimmer J. 1975. Crossed pathways from the entorhinal area to the fascia dentata. I. Normal in rabbits. J Comp Neurol 161:57–70.

Horn G, Bradley P, McCabe BJ. 1985. Changes in the structure of synapse associated with learning. J Neurosci 5:3161–3168.

Howard CV, Reed MG. 1998. Unbiased stereology: three-dimensional measurement in microscopy. Oxford: Bios Scientific.

Howell DC. 1982. Statistical methods for psychology, 2nd ed. Boston: PWS-Kent.

Hunter A, Stewart MG. 1989. A quantitative analysis of the synaptic development of the lobus parolfactorius of the chick (*Gallus domesticus*). Exp Brain Res 78:425–434.

Isaac JTR, Nicoll RA, Malenka RC. 1995. Evidence for silent synapses: implications for the expression of LTP. Neuron 15:427–434.

Kennedy MB. 1998. Signal transduction molecules at the glutamatergic postsynaptic membrane. Brain Res Rev 26:243–257.

Kim JJ, Clark RE, Thompson RF. 1995. Hippocampectomy impairs the memory of recently, but not remotely, acquired trace eyeblink conditioned responses. Behav Neurosci 109:195–203.

Kleim JA, Lussing E, Schwarz ER, Comery TA, Greenough WT. 1996. Synaptogenesis and fos expression in the motor cortex of the adult rat after motor skill learning. J Neurosci 16:4529–4535.

Kleim JA, Vij K, Ballard DH, Greenough WT. 1997. Learning-dependent synaptic modifications in the cerebellar cortex of the adult rat persist for at least four weeks. J Neurosci 17:717–721.

Konorski J. 1948. Conditioned reflexes and neuron organization. Cambridge: Cambridge University Press.

Lee KS, Schottler F, Oliver M, Lynch G. 1980. Brief bursts of high-frequency stimulation produce two types of structural change in rat hippocampus. J Neurophysiol 44:247–258.

Liao D, Hessler NA, Malinow R. 1995. Activation of postsynaptically silent synapses during pairing-induced LTP in CA1 region of hippocampal slice. Nature 375:400–404.

Lorente de Nó R. 1934. Studies on the structure of the cerebral cortex. II. Continuation of the study of the ammonic system. J Psychol Neurol 46:113–177.

Malenka RC, Nicoll RA. 1997. Silent synapses speak up. Neuron 19:473–476.

Mayhew TM, Gundersen HJG. 1996. "If you assume, you can make an ass out of u and me": a decade of the disector for stereological counting of particles in 3D space. J Anat 188:1–15.

Moser M-B, Trommald M, Anderson P. 1994. An increase in dendritic spine density on hippocampal CA1 pyramidal cells following spatial learning in adult rats suggests the formation of new synapses. Proc Natl Acad Sci USA 91:12673–12675.

Moser M-B, Trommald M, Egeland T, Anderson P. 1997. Spatial training in a complex environment and isolation alter the spine distribution differently in rat CA1 pyramidal cells. J Comp Neurol 380:373–381.

Moyer JR Jr, Deyo RA, Disterhoft JF. 1990. Hippocampectomy disrupts trace eye-blink conditioning in rabbits. Behav Neurosci 104:243–252.

Moyer JR Jr, Thompson LT, Disterhoft JF. 1996. Trace eyeblink conditioning increases CA1 excitability in a transient and learning-specific manner. J Neurosci 16:5536–5546.

Nusser Z, Lujan R, Laube G, Roberts JDB, Molnar E, Somogyi P. 1998. Cell type and pathway dependence of synaptic AMPA receptor number and variability in the hippocampus. Neuron 21:545–559.

O'Malley A, O'Connel C, Regan CM. 1998. Ultrastructural analysis reveals avoidance conditioning to induce a transient increase in hippocampal dentate spine density in the 6 h post-training period of consolidation. Neuroscience 87:607–613.

Petralia RS, Esteban JA, Wang Y-X, Partridge JG, Zhao H-M, Wenthold RJ, Malinow R. 1999. Selective acquisition of AMPA receptors over postnatal development suggests a molecular basis for silent synapses. Nature Neurosci 2:31–36.

Power JM, Thompson LT, Moyer JR Jr, Disterhoft JF. 1997. Enhanced synaptic transmission in CA1 hippocampus after eyeblink conditioning. J Neurophysiol 78:1184–1187.

Ramón y Cajal S. 1893. Neue Darstellung vom histologischen Bau des Centralnervensystem. Arch Anat Physiol 319–428.

Royet J-P. 1991. Stereology: a method for analyzing images. Prog Neurobiol 37:433–474.

Rusakov DA, Davies HA, Harrison E, Diana G, Richter-Levin G, Bliss TVP, Stewart MG. 1997. Ultrastructural synaptic correlates of spatial learning in rat hippocampus. Neuroscience 80:69–77.

Schuster T, Krug M, Wenzel J. 1990. Spinules in axospinous synapses of the rat dentate gyrus: changes in density following long-term potentiation. Brain Res 523:171–174.

Solomon PR, Van der Schaaf EV, Thompson RF, Weisz DJ. 1986. Hippocampus and trace conditioning of the rabbit's classically conditioned nictitating membrane response. Behav Neurosci 100:729–744.

Sterio DC. 1984. The unbiased estimation of number and sizes of arbitrary particles using the disector. J Microsc (Lond) 134:127–136.

Stewart MG, Csillag A, Rose SPR. 1987. Alterations in synaptic structure in the paleostriatal complex of the domestic chick, *Gallus domesticus*, following passive avoidance training. Brain Res 426:69–81.

Stewart MG, Rusakov DA. 1995. Morphological changes associated with stages of memory formation in the chick following passive avoidance training. Behav Brain Res 66:21–28.

Takumi Y, Ramirez-Leon V, Laake P, Rinvik E, Ottersen OP. 1999. Different modes of expression of AMPA and NMDA receptors in hippocampal synapses. Nature Neurosci 2:618–624.

Tanzi E. 1893. I fatti i le induzioni nell'odierna istologia del sistema nervoso. Riv Sperim Freniatr Med Leg 19:419–472.

Van der Zee EA, Kronforst-Collins MA, Maizels ET, Hunziger-Dunn M, Disterhoft JF. 1997. γ isoform-selective changes in PKC immunoreactivity after trace eyeblink conditioning in the rabbit hippocampus. Hippocampus 7:271–285.

Van Reempts J, Dikova M, Webrouck L, Clincke G, Borgers M. 1992. Synaptic plasticity in rat hippocampus associated with learning. Behav Brain Res 51:179–183.

Vrensen G, Nunes Cardozo J. 1981. Changes in size and shape of synaptic connections after visual training: an ultrastructural approach to synaptic plasticity. Brain Res 218:79–97.

Wallenstein GV, Eichenbaum H, Hasselmo ME. 1998. The hippocampus as an associator of discontiguous events. Trends Neurosci 21:317–323.

Weibel ER. 1979. Stereological methods, vol 1. Practical methods for biological morphometry. New York: Academic Press.

Wenzel J, Kammerer E, Kirsche W, Matthies H, Wenzel M. 1980. Electron microscopic and morphometric studies on the synaptic plasticity in the hippocampus of the rat following conditioning. J Hirnforsch 21:647–654.

West MJ. 1993. New stereological methods for counting neurons. Neurobiol Aging 14:275–285.

West MJ. 1999. Stereological methods for estimating the total number of neurons and synapses: issues of precision and bias. Trends Neurosci 22:51–61.

Ziff EB. 1997. Enlightening the postsynaptic density. Neuron 19:1163–1174.